Cancer Cell
Article

Low-Dose Irradiation Programs Macrophage Differentiation to an iNOS$^+$/M1 Phenotype that Orchestrates Effective T Cell Immunotherapy

Felix Klug,[1,11] Hridayesh Prakash,[1,2,4,11] Peter E. Huber,[5,11,*] Tobias Seibel,[1,11] Noemi Bender,[1] Niels Halama,[6] Christina Pfirschke,[1] Ralf Holger Voss,[7] Carmen Timke,[5] Ludmila Umansky,[1] Kay Klapproth,[8] Knut Schäkel,[2] Natalio Garbi,[9,10] Dirk Jäger,[6] Jürgen Weitz,[3] Hubertus Schmitz-Winnenthal,[3] Günter J. Hämmerling,[8] and Philipp Beckhove[1,*]
[1]Division of Translational Immunology, German Cancer Research Center (DKFZ) and National Center of Tumor Diseases (NCT), 69120 Heidelberg, Germany
[2]Department of Dermatology, Heidelberg University Medical Center, 69120 Heidelberg, Germany
[3]Department of Visceral Surgery, Heidelberg University Medical Center, 69120 Heidelberg, Germany
[4]Department of Biochemistry, School of Life Sciences, University of Hyderabad, Hyderabad 500046, India
[5]Department of Molecular and Radiation Oncology, DKFZ and Heidelberg University Medical Center, 69120 Heidelberg, Germany
[6]Department of Medical Oncology, NCT, Heidelberg University Medical Center, 69120 Heidelberg, Germany
[7]Department of Hematology, University Hospital of Mainz, 55131 Mainz, Germany
[8]Division of Cellular Immunology, DKFZ, 69120 Heidelberg, Germany
[9]Division of Molecular Immunology, DKFZ, 69120 Heidelberg, Germany
[10]Institutes of Molecular Medicine and Experimental Immunology, University of Bönn, 53113 Bonn, Germany
[11]These authors contributed equally to this work
*Correspondence: p.huber@dkfz.de (P.E.H.), p.beckhove@dkfz.de (P.B.)
http://dx.doi.org/10.1016/j.ccr.2013.09.014

SUMMARY

Inefficient T cell migration is a major limitation of cancer immunotherapy. Targeted activation of the tumor microenvironment may overcome this barrier. We demonstrate that neoadjuvant local low-dose gamma irradiation (LDI) causes normalization of aberrant vasculature and efficient recruitment of tumor-specific T cells in human pancreatic carcinomas and T-cell-mediated tumor rejection and prolonged survival in otherwise immune refractory spontaneous and xenotransplant mouse tumor models. LDI (local or pre-adoptive-transfer) programs the differentiation of iNOS$^+$ M1 macrophages that orchestrate CTL recruitment into and killing within solid tumors through iNOS by inducing endothelial activation and the expression of TH1 chemokines and by suppressing the production of angiogenic, immunosuppressive, and tumor growth factors.

INTRODUCTION

Intrinsic resistance of tumors to effector T cell infiltration is a major hurdle to successful tumor immune rejection. Low T cell infiltrates are predictive of poor prognosis in many human cancers (Fridman et al., 2011) and failure of response to cancer immunotherapy treatment (Halama et al., 2011). Even high numbers of fully activated tumor-specific CD4$^+$ TH1 and cytotoxic CD8$^+$ T cells can fail to reject established, immunogenic murine or human tumors due to their insufficient recruitment to tumor tissue (Ganss and Hanahan, 1998; Ganss et al., 2002; Garbi et al., 2004). A key impediment for T cell extravasation into tumors is the establishment of an aberrant vasculature (Hamzah et al., 2008).

Ongoing production of angiogenic growth factors in tumors induces profound morphological and molecular changes in tumor blood vessels (Ryschich et al., 2002; St Croix et al., 2000). This process, underlying the tumor's intrinsic resistance to lymphocytic infiltration and immune surveillance, has been termed tumor endothelial cell anergy (Griffioen et al., 1996).

Significance

We here demonstrate that iNOS$^+$ macrophages in the tumor microenvironment are both required and sufficient to mediate effector T cell recruitment into tumor tissue and successful tumor immune rejection through an NO-dependent mechanism, thereby representing indispensable components of future immunotherapeutic strategies. INOS expression in murine and human tumor-infiltrating macrophages was induced by local low-dose irradiation that can be easily applied in clinical settings. Adoptive transfer of iNOS-expressing macrophages may also represent a promising intervention to establish those populations of macrophages in the tumor tissue that enable therapeutic efficacy of cancer immunotherapy.

Endothelial anergy can be studied in the RIP1-Tag5 (RT5) mouse model of spontaneous pancreatic islet carcinogenesis. The oncogene SV40-Tag (Simian Virus 40 large T antigen) is induced in the beta cells of pancreatic islets under the control of the rat insulin promoter (RIP) in RT5 mice at the age of 10 weeks (Hanahan, 1985), resulting in highly vascularized, invasive tumors within 20 weeks. Invasive tumor growth leads to progressive insulin secretion, causing hypoglycemic death within 30 weeks (Ganss and Hanahan, 1998).

Functional SV40-Tag-specific cytotoxic lymphocytes can be generated throughout tumor development and preneoplastic lesions are infiltrated by Tag-specific T cells (Ganss and Hanahan, 1998). However, endogenous or adoptively transferred tumor antigen-reactive T cells lose the capacity to infiltrate malignant tissue during tumor progression (Ryschich et al., 2002). At this stage, RT5 tumors are characterized by morphological anomalies of blood vessels, the appearance of hemorrhages, and impaired leukocyte attachment to the endothelium. Therapeutic options to overcome this barrier and to support T cell infiltration into tumors are limited.

Effective T cell immigration into peripheral tissues occurs at sites of infection-induced inflammation through interaction with endothelial cells and is guided by chemokines secreted by activated cells of the innate immune system (Motz and Coukos, 2011). Such conditions can be induced by inflammatory stimuli, such as toll-like receptor (TLR) agonists (Garbi et al., 2004). However, their systemic administration may result in generalized tissue inflammation posing a high risk of life-threatening side effects. Low-risk therapeutic procedures for cancer tissue targeted T cell recruitment therefore need to be developed. Radiotherapy is the only clinically advanced approach for noninvasive, site-specific intervention. Local radiotherapy has lately been discussed in the context of its capacity to support the induction and function of tumor-specific T cells through antigen release from dying tumor cells together with an activation of antigen-presenting cell subsets (Antonia et al., 2004; Tesniere et al., 2008). However, local radiotherapy may also possess the potential to support T cell immigration. In RT5 mice, sublethal total body irradiation followed by bone marrow transplantation permitted RT5 tumors to be infiltrated by adoptively transferred, tumor antigen-specific effector T cells and resulted in normalization of the tumor vasculature and complete rejection of well-established tumors (Cao et al., 2002; Ganss et al., 2002). We exploited the RT5 tumor model, human melanoma xenografts, and human pancreatic cancer specimens from patients receiving low-dose irradiation (LDI) in the setting of a controlled clinical trial to assess whether local radiotherapy can be used as an adjuvant to improve the efficacy of adoptive T cell therapy or tumor vaccination.

RESULTS

Local LDI Induces Recruitment of Tumor-Specific T Cells into Insulinomas

We first irradiated the pancreatic regions (Figure S1A available online) of otherwise untreated RT5 mice at 24 weeks of age with single doses of 0.5–6 Gy, when tumors had already invaded surrounding pancreatic tissue (Figure 1A). After 7 days, irradiated tumors contained up to four times the number of T cells (Figure 1B). These were highest after application of 0.5 Gy and accompanied by an increase of CD4$^+$ FoxP3$^+$ T cells (Figure S1B). At higher doses of 1, 2 and 6 Gy, T cell infiltration gradually declined to baseline levels, most likely due to dose-dependent lymphopenia attributed to concomitant irradiation of the spleen (data not shown).

We transferred 5×10^6 activated tag-specific TCR transgenic CD8$^+$ (TCRCD8$^+$) or CD4$^+$ (TCRCD4$^+$) effector T cells i.p. into 24-week old RT5 mice (Figure 1C) to specifically study the immigration of tumor antigen-specific effector T cell populations. While in both settings T cells only scarcely infiltrated unirradiated tumors, they strongly immigrated into irradiated RT5 tumors (Figures 1D and 1E). Accumulation of TCRCD8$^+$ T cells and, to a lesser extent, TCRCD4$^+$ T cells in irradiated tumors triggered a concomitant immigration of host-derived CD4$^+$ and CD8$^+$ (Figure 1E), FoxP3$^+$ T (Figures S1B–S1D; Nummer et al., 2007) and CD11b$^+$ cells (Figure 1D; Figure S1E). We used a dose of 2 Gy for most of the subsequent experiments because it provided the highest ratio of effector T cells to FoxP3$^+$ immunosuppressive regulatory T cells when combined with adoptive T cell transfer.

Local LDI did not only trigger tumor immigration of transferred high-affinity T cells, but also enabled accumulation of tag-specific endogenous CD8$^+$ T cells that were induced through tag-specific prime-boost vaccinations with an MHC-I restricted tag epitope (SEFLLEKRI) 1 week before and after irradiation in 24-week-old RT5 mice under the immunosuppressive influence of their large tumors (Griffioen et al., 1996; Figure 1F).

We next challenged the possibility that the observed T cell accumulation was caused by unintended co-irradiation of neighboring tissues such as the spleen or surrounding nonmalignant pancreatic tissue. Irradiation-induced tumor infiltration by transferred T cells was not impaired in splenectomized RT5 mice (Figure S1F). This effect was also observed in RT5 insulinomas that were subcutaneously transplanted into the flank region of NOD/Scid mice, where they grew progressively in the absence of the specific pancreatic microenvironment (Figure S1G).

In summary, these findings demonstrate that local LDI promotes infiltration of large, established tumors by T cells through direct radiation effects on the tumor tissue irrespective of the tumor localization or local microenvironment.

Local LDI Promotes Normalization of Aberrant Vasculature, T Cell-Mediated Tumor Rejection, and Survival

Insulinomas in 24-week-old RT5 mice show an aberrant tumor vasculature characterized by the presence of hemorrhagic lesions and dilated tumor vessels and preventing T cell entry (Hamzah et al., 2008). Normalization of the tumor vasculature is thus a hallmark of efficient T cell therapy in RT5 mice.

We observed a normalization of the tumor vasculature in animals treated with a combination of LDI and adoptive TCRCD8$^+$ T cell transfer. This was indicated by a reduction in the CD31$^+$ vessel area, average vessel size, and hemorrhagic lesions (Figures 2A–2C), as well as by an increase of the vessel circularity index (Figure 2C) in a majority of tumors that was not detectable upon T cell transfer into unirradiated mice (Figures 2A and 2B). Importantly, CD8$^+$ TC transfer into irradiated tumors also caused a massive activation of the tumor vasculature, as indicated by

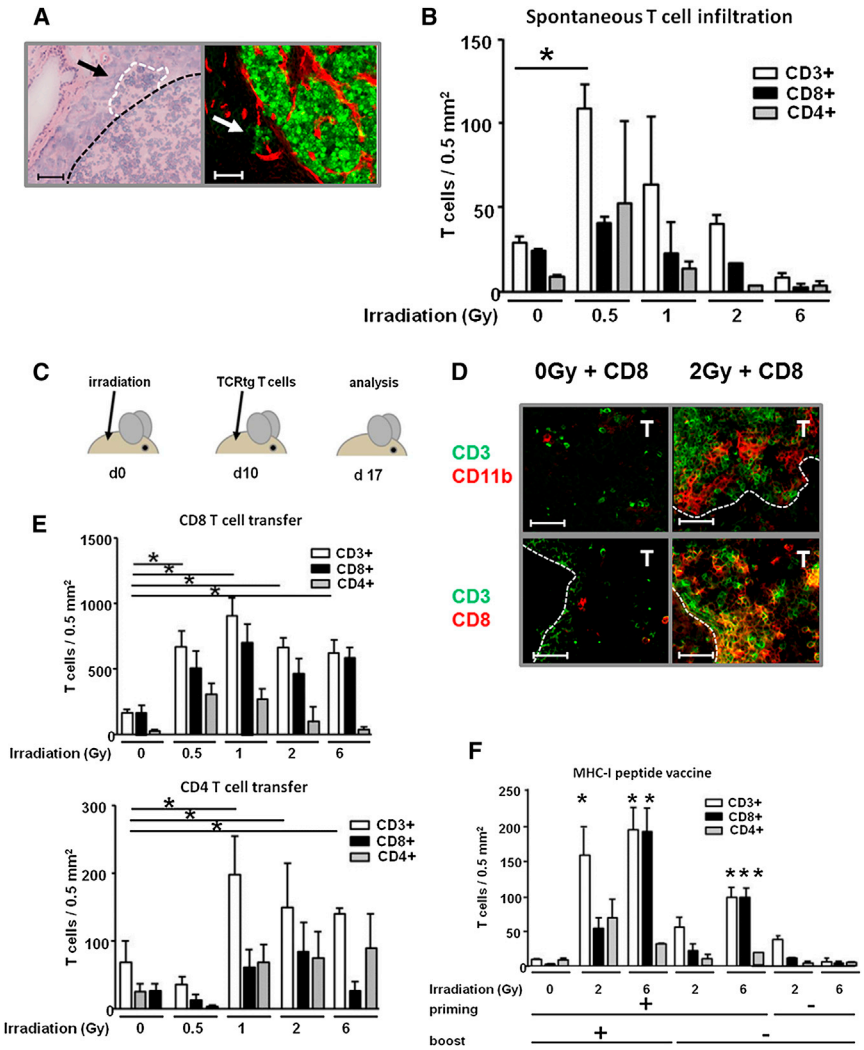

Figure 1. Increased T Cell Infiltration after Local LDI

(A) Invasive growth of RT5 tumors in 24-week-old mice. Left: hematoxylin and eosin (H&E) staining; right: IHC costaining of tumor cells (Tag: green) and endothelial cells (CD31: red). Scale bar, 50 μm.

(B) Tumor infiltration by host T cells. Tumors of RT5 mice (n = 8) were treated with indicated irradiation doses and analyzed after 7 days with immunohistochemistry (IHC) for indicated T cell populations.

(C) Schematic experimental procedure for combined LDI and adoptive transfer of Tag-specific TCRtg T cells.

(D) Increased infiltration of myeloid CD11b$^+$ and transferred CD3$^+$ or CD8$^+$ T cells, or both, in intratumoral areas of LD-irradiated RT5 tumors (IHC). Tumor areas are indicated (T) and delineated (dashed lines). Magnification: 200×.

(E) Tumor infiltration by TCRCD8$^+$ (n = 22, upper graph) or TCRCD4$^+$ (n = 13, lower graph) T cells analyzed by IHC for indicated T cell populations.

(F) Tumor T cell infiltration 7 days after vaccination with MHC-I restricted SV40-Tag peptide and LD irradiation at indicated doses. Mean ± SEM are shown. *$p < 0.05$ (two-tailed Student's t test). See also Figure S1.

expression of VCAM-1 (Figure 2C) required for leukocyte recruitment into inflamed tissue.

However irradiation or T cell transfer, or both, did not induce the formation of high endothelial venules because the subsequent endothelial lining remained consistently flat. Vascular normalization occurred only in conjunction with the transfer of CD8$^+$ T cells, because irradiation alone (data not shown) or the transfer of TCRCD4$^+$ T cells had a much weaker effect on the tumor vasculature (Figure 2B).

This led us to ask whether a combination of local LDI and CD8$^+$ T cell transfer would result in rejection of RT5 tumor cells and the improved survival of mice carrying large RT5 tumors. We therefore irradiated 24-week-old RT5 mice with a single dose of 2 Gy followed by repeated applications of 5×10^6 TCRCD8$^+$ T cells (Figure 2D). This treatment resulted in significant tumor reduction (Figure 2E) and long-term survival of all animals over the entire observation period of 52 weeks. In contrast, mice treated with T cell transfer alone showed only a slight increase in overall survival and died within 42 weeks (Figure 2D).

To determine T cell mediated tumor cell rejection in RT5 mice after the T cell transfer, we quantified the development of blood glucose levels (which inversely correlate with the number of viable insulinoma cells) after a single T cell transfer (Garbi et al., 2004). Glucose levels gradually declined after treatment with 2 Gy or transfer of TCRCD8$^+$ or TCRCD4$^+$ T cells alone, indicating progressive tumor growth. In contrast, T cell transfer into low-dose-irradiated animals caused a significant increase and normalization of blood glucose over 5–6 weeks (Figure S2), indicating transient tumor cell destruction.

Local LDI Improves Immunotherapy of Human Melanoma

We next tested whether local LDI would also support T cell therapy of human tumors. To this end, we xenotransplanted the HLA-A2 positive human melanoma cell line MeWo i.d. into the lower hind leg of NSG mice. MeWo cells express the melanoma antigen gp-100 and form progressive tumors after transplantation. After 6 days, established tumors were locally irradiated with 2 Gy and 1 day later each mouse was treated intravenously (i.v.) with 2.5×10^6 purified human T cells that were transduced with a human HLA-A2 restricted gp-100-specific TCR and exerted strong cytotoxic activity against MeWo cells in vitro (Voss et al., 2010; our data not shown). Melanomas were removed and analyzed for T cell infiltration 15–17 days after the T cell transfer. Irradiated tumors were consistently infiltrated by varying proportions of transferred human cells, unlike unirradiated tumors (Figure 3A). Moreover, we observed that a combined treatment of tumor irradiation and subsequent T cell

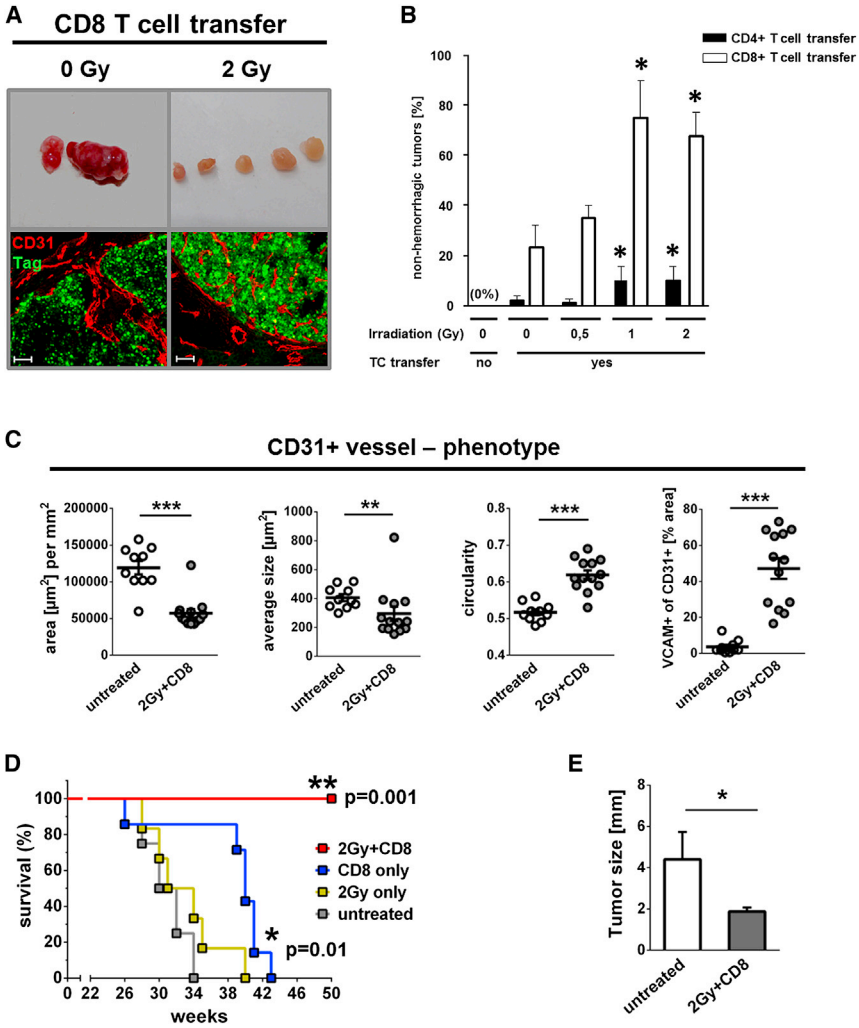

Figure 2. Treatment Response after Local LDI

(A and B) Normalization of tumor vasculature. RT5 mice (n = 40) were treated with LDI at indicated doses and received TCRCD8$^+$ or TCRCD4$^+$ T cells as indicated after 10 days. Tumors were analyzed 1 week later. (A) Upper panel: representative RT5 tumors with hemorrhagic (no irradiation; 0 Gy) and nonhemorrhagic tumors (irradiation; 2 Gy). Lower panel: IHC of tumor vasculature with anti-CD31 mAb (red). Tumor cells are labeled with Tag-specific mAb (green). Scale bar, 50 µm. (B) Mean ± SEM proportion of nonhemorrhagic tumors per animal are shown.

(C) Phenotype of CD31$^+$ vessels. Area per square millimeter, average size, circularity, and vessel activation status—defined by VCAM + CD31$^+$ vessels—of CD31$^+$ tumor vessels in untreated mice (analyzed tumors = 10) and mice treated with LDI (2 Gy) + TC (CD8) (analyzed tumors = 13). Individual groups consisted of two mice.

(D) Survival of RT5 mice. Individual groups of four to seven 24-week-old, large tumor-bearing mice received a single dose of LDI (2 Gy at week 24), followed 10 days later by applications of 5 × 10^6 TCRCD8$^+$ T cells at weekly intervals during the first 5 weeks and biweekly intervals thereafter (2 Gy + CD8). Control groups were untreated or received T cell transfers only (CD8) or LDI (2 Gy) only. The significance of the survival curves between the groups 2 Gy + CD8 and untreated were tested with the Mantel-Cox test. **$p < 0.01$ (Mantel-Cox test).

(E) Mean ± SEM tumor size of untreated mice and mice treated with LDI (2 Gy) + TC (CD8). Individual groups consisted of three to five mice with five to nine tumors. Mean ± SEM are shown. *$p < 0.05$; **$p < 0.01$; ***$p < 0.001$ (two tailed Student's t test). See also Figure S2.

transfer resulted in efficient inhibition of tumor outgrowth, while irradiation or T cell transfer alone had no effect on melanoma progression in this set-up (Figure 3B).

Local LDI was thus required for the accumulation of tumor-specific T cells in human melanomas and efficient human melanoma immunotherapy.

T Cell Recruitment Is Mediated by Irradiated Tumor-Infiltrating Macrophages

We next dissected those cell types whose activation through LDI-mediated vascular normalization and T cell recruitment. We focused on tumor-infiltrating macrophages because T cell infiltration in RT5 tumors was found to be accompanied by macrophage accumulation (Ganss et al., 2002). TAMs essentially contribute to aberrant tumor angiogenesis and may thus regulate antitumor immune responses after irradiation (Motz and Coukos, 2011). CD11b$^+$ cells in untreated RT5 tumors largely co-expressed F4/80 and CD68 (Figure S3A), demonstrating their TAM nature. We selectively deleted tissue-resident macrophages and their monocytic precursors (subsequently summarized under the term "macrophages" for simplification) in 24-week-old, tumor-bearing animals with weekly injections of clodronate-loaded liposomes (CLIP; Zeisberger et al., 2006). This treatment profoundly reduced the numbers of macrophages in the spleen, tumor, and pancreas (Figure S3B; data not shown). Tumors were irradiated 3 days after the first CLIP application and animals were treated with a single injection of TCRCD8$^+$ or TCRCD4$^+$ T cells 10 days later. CLIP treatment completely inhibited T cell recruitment into irradiated tumors (Figures 4A and 4B). CLIP application also prevented the normalization of blood glucose levels (Figure S3C) and completely abrogated the positive effect of irradiation on survival after repeated TCRCD8$^+$ T cell transfers (Figure 4C, compare with Figure 2C). Thus, tumor-infiltrating macrophages are not only involved in the suppression of antitumor immune responses but can also function as essential mediators of efficient T cell recruitment into irradiated RT5 tumors and for efficient tumor immune rejection. In this regard, it is interesting to note that in late stage RT5 tumors, CLIP application alone without additional immunotherapy had no influence on vascular phenotype, tumor size, or survival when compared to untreated mice (Figures 4C and S3D–S3F).

We next investigated whether irradiation directly targeted macrophages and whether they required the context of an irradiated tumor microenvironment to mediate tumor T cell

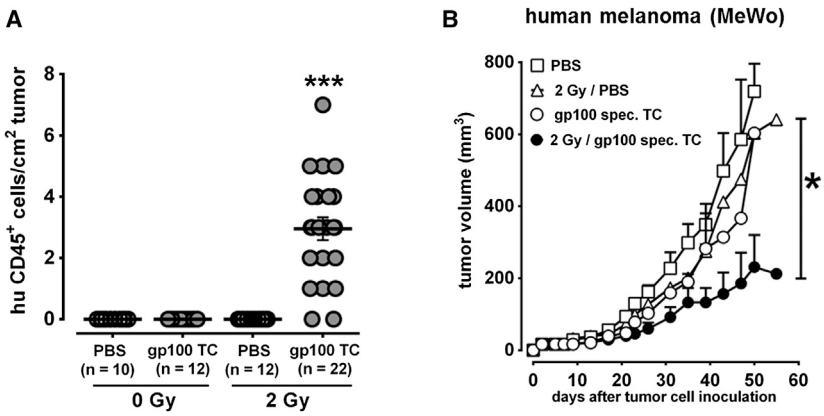

Figure 3. Local LDI Improves Immunotherapy of Human Melanoma

(A) Infiltration of xenotransplanted MeWo cells by transferred human gp100 TCR-transduced T cells after LDI with 2 Gy. All test animals carried established melanomas of 6–8 mm diameter before LDI. Ten days after irradiation animals were treated i.v. with 2.5×10^6 gp100 TCR-transduced T cells per mouse. Control mice did not receive T cells (PBS) or irradiation (0 Gy), or both. Human $CD45^+$ cells were quantified 15–17 days later with IHC. Dots represent cell numbers per analyzed area; n, number of analyzed tissue slides; and TC, T cells.

(B) Control of human melanoma outgrowth by gp100 TCR-transduced T cells after LDI. Animals were engrafted i.d. with human MeWo melanoma cells. Tumors were irradiated after 6 days with 2 Gy LDI and treated with 2.5×10^6 gp100 specific T cells per mouse 1 day later. Mean ± SEM tumor volume of three animals per group are shown for the test group (black circles) and for control groups that were left untreated (PBS; white squares), or received irradiation (2 Gy/PBS; white triangles) only or T cell transfer (gp100 spec. TC; white circles) only. *$p < 0.05$; ***$p < 0.001$ (two-tailed Student's t test).

recruitment. To this end, we isolated peritoneal macrophages from 2 Gy total body irradiated (or unirradiated) syngeneic wild-type (WT) donor mice and transferred a dose per mouse of 5×10^6 of them i.v. into unirradiated 24-week old, tumor-bearing RT5 mice 10 days before $TCRCD8^+$ T cell transfer (Figure S4A). The majority of isolated peritoneal cells was $CD11b^+$, while only minor proportions were $Gr\text{-}1^+$. In the $Gr\text{-}1^-$ population, 77%–82% expressed CD11b and 92%–95% of them were CD11c negative or low (Figure S4B), thus containing only few dendritic cells. Treatment of unirradiated mice with irradiated macrophages and $TCRCD8^+$ T cells resulted in full remission of hemorrhages (Figures 5A and 5B), efficient tumor size reduction (Figure 5C), and normalization and activation of the tumor vasculature (Figure 5D) accompanied by strong immigration of $CD11b^+$ macrophages and T cells, which accumulated within intratumoral areas in close vicinity to each other (Figure 5E). In contrast, combined treatment with unirradiated macrophages and $TCRCD8^+$ T cell transfer affected neither vascular phenotype nor T cell or macrophage infiltration in intratumoral areas (Figures 5A, 5B, and 5E).

Adoptive cellular transfer caused pronounced changes in the composition of intratumoral myeloid cell infiltrates in RT5 tumors. We detected high infiltrates with $GR1^+$ myeloid cells but only few mature $F4/80^+$ macrophages in tumors that were untreated or treated with $TCRCD8^+$ T cells only (Murray and Wynn, 2011). Cotransfer of irradiated macrophages resulted in an almost complete absence of $Gr1^+$ cells and massive infiltration by $F4/80^+$ macrophages, which was not detectable upon transfer of unirradiated peritoneal cells (Figure 5F). Thus, vascular normalization and T cell recruitment were associated with the intratumoral accumulation of $CD11b^+$ $F4/80^+$ $Gr1^-$ macrophages.

Quantitative analysis revealed major differences between irradiated and unirradiated macrophages with regard to their recruitment to intratumoral areas and peritumoral stroma (Figure 5G). Local tumor irradiation or transfer of irradiated macrophages resulted in macrophage accumulation within intratumoral areas but not peritumorally. In contrast, unirradiated macrophages did not infiltrate intratumoral areas but accumulated within peritumoral stroma (Figure S4C). While transfer of irradiated macrophages resulted in strong intratumoral accumulation of $CD3^+$, $CD8^+$, and $CD4^+$ T cells, transfer of unirradiated macrophages had no effect on tumor T cell infiltration (Figure 5H).

In summary, these data demonstrate that LDI-induced vascular normalization, T cell recruitment, and tumor immune rejection in RT5 tumors require TAMs and are correlated with intraepithelial macrophage accumulation and reduced infiltration of $Gr1^+$ myeloid cells.

iNOS Expression Is Required for T Cell Recruitment by Tumor-Infiltrating Macrophages

Macrophage activation results in two broader functional categories. M1-like macrophages are induced by TH1 polarizing cytokines. They are characterized by secretion of interleukin-12 (IL-12), the expression of iNOS, and possess the capacity to clear infections and support TH1 immune responses (Murray and Wynn, 2011). Alternatively activated macrophage subsets (commonly summarized as M2 macrophages) respond to TH2 cytokines and are strongly enriched in tumors. By activation of M2-associated transcription factors HIF-1, Ym-1, Fizz-1, and arginase (Gordon and Martinez, 2010; Motz and Coukos, 2011), they are endowed with trophic functions of wound healing, fibrosis, angiogenesis, promotion of TH2-mediated humoral immune responses, and the capacity to suppress TH1-mediated immunity. This subset secretes IL-10 and vascular endothelial growth factor (VEGF) and contributes essentially to tumor progression and suppression of antitumor immunity (Murray and Wynn, 2011).

We hypothesized that T cell recruitment into irradiated RT5 tumors may be mediated by $iNOS^+$ tumor-infiltrating macrophages induced by LDI. To test this hypothesis, we first characterized the expression of iNOS and M2-associated parameters such as HIF-1, Ym-1, Fizz-1, and arginase in $CD11b^+$ peritoneal macrophages from tumor-bearing RT5 mice that were either untreated or subjected to 2 Gy total body irradiation with western blot analysis. Unirradiated populations expressed M2-associated transcription factors but minor amounts of iNOS (Figure 6A), corresponding to an M2 phenotype. In contrast, 2 Gy local tumor

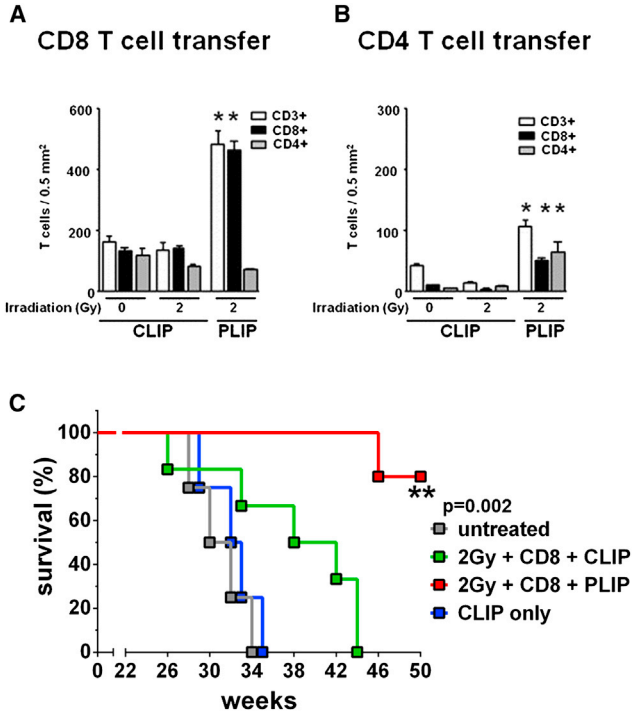

Figure 4. Tumor Infiltration by Transferred TCRtg T Cells Is Abrogated by Depletion of Macrophages

(A and B) RT5 mice (n = 15) were given repeated injections of clodronate (CLIP) or saline (PLIP) loaded liposomes i.p. starting 1 week before treatment with 2 Gy local LDI and i.p. injections of TCRCD4$^+$ (A) or TCRCD8$^+$ (B) T cells, respectively. Tumors were analyzed 1 week later by IHC for infiltration with indicated T cell subsets. Mean ± SEM. T cell numbers/0.5 mm^2 are shown. *$p < 0.05$ (two-tailed Student's t test).

(C) Survival of RT5 mice. Individual groups of four to seven 24-week-old, large tumor-bearing mice received a single dose of LDI (2 Gy at week 24), followed 10 days later by applications of 5×10^6 TCRCD8$^+$ T cells at weekly intervals during the first 5 weeks and biweekly intervals thereafter with or without macrophage ablation by applications of clodronate- (2 Gy + CD8 + CLIP) or saline- (2 Gy + CD8 + PLIP) loaded liposomes, respectively. Control groups were untreated or received applications of clodronate-loaded liposomes every 5 days (CLIP only). The significance of the survival curves between the groups 2 Gy + CD8 + CLIP and 2 Gy + CD8 + PLIP were tested with the Mantel-Cox test. **$p < 0.01$ (Mantel-Cox test).

See also Figure S3.

irradiation simultaneously induced iNOS expression and a reduction in HIF-1, Ym-1, Fizz-1, and arginase expression in this population (Figure 6A), indicating an irradiation-induced acquisition of an M1 phenotype. Indeed, in vitro irradiation of isolated RT5 peritoneal macrophages induced iNOS expression (Figure 6B) and in vitro LDI of both peritoneal and isolated RT5 tumor-infiltrating macrophages caused increased NO secretion (Figure 6C). In summary, these data demonstrate that LDI induces iNOS expression and increases NO secretion in macrophages.

We next analyzed the expression of iNOS in CD11b$^+$ tumor-infiltrating macrophages after adoptive T cell transfer by immunohistochemistry. While iNOS expression was undetectable in unirradiated tumors, 15% of CD11b$^+$ cells in locally irradiated tumors expressed iNOS (Figures 6D and 6E). These were often clustered (Figure 6E) in the vicinity of T cell infiltrates but also scattered throughout RT5 tissues (not shown). Importantly, total body irradiation also increased iNOS expression in peritoneal CD11b$^+$ CD11c^{low} Gr1^{low} inflammatory monocytes and in CD11b$^+$ CD11c^{high} monocytes but not in CD11b− peritoneal cells from C3H donor mice and Gr-1$^+$ cells (Figure 6F; data not shown). Upon transfer of these cells into unirradiated tumor-bearing mice 10% of tumor-infiltrating CD11b$^+$ cells expressed iNOS, while in mice receiving unirradiated macrophages iNOS remained undetectable (Figure 6E).

To assess whether iNOS activity is essential for vascular normalization, activation, and T cell recruitment into RT5 tumors, we treated tumor-bearing mice with the highly specific iNOS inhibitor, N-(3-(aminomethyl)benzyl)acetamidine (1400W; Garvey et al., 1997) prior to local 2 Gy tumor irradiation and TCRCD8$^+$ T cell transfer. The 1400W treatment reduced NO secretion in irradiated and CD8TC-treated tumors to undetectable levels (Figure S5A). Upon iNOS inhibition, reduction in CD31$^+$ endothelial cells was only partially blocked but vascular cell adhesion protein-1 (VCAM-1) expression, indicating endothelial cell activation and the capacity to support leukocyte transmigration, was almost completely inhibited (Figure 6G).

Accordingly, upon iNOS inhibition, recruitment of T cells, CD11b$^+$, and CD68$^+$ macrophages into irradiated tumors as well as tumor rejection were completely abrogated (Figures 6H, S5B, and S5C), while tumor infiltration by Gr-1$^+$ myeloid cells was fully restored to the levels of untreated mice (Figure S5B).

Irradiated Macrophages and iNOS Control Tumorigenic Cancer Inflammation

Recent observations suggest that tumor-promoting functions of TAMs are driven by a common program resulting in increased angiogenesis and inflammation, and reduced antitumor immunity (Motz and Coukos, 2011). This program is reflected by increased expression of characteristic cytokines, chemokines, and growth factors in the tumor microenvironment, involving TH2 cytokines (including IL-6), TH2 chemokines, VEGF, and granulocyte-macrophage colony-stimulating factor (GM-CSF). However, we have shown that iNOS$^+$ macrophages are indispensable to tumor immune rejection. To understand how irradiation affected TAM-dependent immunomodulatory processes in the tumor microenvironment, we quantified factors associated with tumor-promoting TAM activity or protective antitumor immunity in the tumor tissue of treated and untreated 24-week-old RT5 mice using Luminex analysis.

In untreated RT5 tumors, the TH2 cytokines IL-4, IL-5, IL-6, IL-9, and IL-10 were low and not affected by treatment with local LDI alone. Sample results for IL-10 and IL-5, and cumulative results for all TH2 cytokines are shown in Figure 7A. In contrast, adoptive transfer of activated TCRCD8$^+$ cells into unirradiated tumors resulted in a strong increase in all tested TH2 cytokines, demonstrating a hitherto unexpected, potentially reversing effect of adoptive cellular immunotherapy. The increase in TH2 cytokines after T cell transfer was mediated by TAMs because it was abrogated by CLIP treatment. Remarkably TH2 induction was completely (IL-4 and IL-13) or markedly (IL-5, IL-6, IL-9, and IL-10) inhibited in irradiated tumors. This inhibition was completely (IL-9, IL-10, and IL-13) or partially (IL-4, IL-5, and IL-6) mediated by iNOS, because iNOS inhibition restored TH2 cytokine expression even in irradiated tumors. These

observations suggest that TAM-induced TH2 cytokine expression in T cell-treated, late-stage RT5 tumors is inhibited by irradiated (iNOS+) macrophages. This hypothesis was confirmed by our finding that adoptively transferred, irradiated macrophages suppressed TH2 cytokine induction in unirradiated tumors to a similar degree as local LDI (Figure 7A). In contrast to TH2 cytokines, TH1 cytokine expression such as IL-12 or interferon (IFN)-gamma was not inhibited by tumor irradiation, iNOS, or transfer of irradiated macrophages (Figure 7B).

We next assessed the impact of irradiation, iNOS, and TAMs on the concentration of a major TH1 recruiting chemokine RANTES and on the balance between RANTES (Islam and Luster, 2012) and the major TH2 cytokine TARC (CCL17; De Monte et al., 2011) in late stage RT5 tumors (Figure 7C). RANTES expression depended on the presence of TAM because it was abrogated after TAM depletion. TARC was strongly upregulated after low-dose tumor irradiation or transfer of irradiated (compared to unirradiated) macrophages into nonirradiated, tumor-bearing mice. Interestingly iNOS inhibition resulted in a marked reduction in RANTES expression, suggesting iNOS affects RANTES-mediated T cell migration. TARC expression was induced to some degree by low dose irradiation alone as well as by adoptive T cell transfer. However, upon combination, both treatments caused a reduction in TARC expression (Figure S6A), resulting in a shift of the TH1–TH2 chemokine balance toward RANTES upon local tumor irradiation or transfer of irradiated macrophages (Figure 7C). The transfer of irradiated macrophages also suppressed the induction of VEGF and GM-CSF in RT5 tumors, which was induced by either treatment with local irradiation or adoptive T cell transfer alone and increased in the absence of iNOS activity (Figures S6B and S6C). Because VEGF and GM-CSF are major inducers of an aberrant vessel phenotype (VEGF) and recruitment of immunosuppressive, myeloid-derived suppressor cells (Bayne et al., 2012), their inhibition by iNOS+ macrophages might play an important role in vessel normalization and improved immunity after local LDI.

In summary, these findings demonstrate that treatment of large, established tumors with activated tumor-specific CD8 T cells alone can trigger the establishment of a TH2 prone, tumor-promoting microenvironment through TAMs, which may contribute to the only limited efficacy of CD8 T cell transfers alone. This can be prevented by local LDI or the adoptive transfer of irradiated macrophages through the induction of iNOS, which suppresses immunosuppressive factors and supports TH1 cell recruitment and activity.

Local LDI of Human Carcinomas Induces iNOS Expression of TAMs and Results in Strong Tumor Infiltration by CD4+ and CD8+ T Cells

Increased intraepithelial T cell infiltrates are correlated with improved survival in patients with pancreatic cancer (De Monte et al., 2011). To assess whether local LDI also increases T cell infiltration into human carcinomas, we compared T cell infiltrates in advanced human pancreatic adenocarcinomas treated in a neoadjuvant setting by single dose local irradiation of 0.5–5 Gy to T cell infiltrates in unirradiated advanced pancreatic cancers 3 days prior to tumor resection within the framework of a controlled clinical study (Timke et al., 2011). T cell infiltration analysis was conducted in a fully automated and blinded manner. Irradiated tumors showed a 3- to 5-fold increase in intraepithelial CD4+ and CD8+ T cells (Figures 8A and 8B) which, in accordance with our observations in RT5 tumors, correlated with a 10-fold reduction in the average intraepithelial vessel size to levels in surrounding nonmalignant stroma areas (Figures 8C and 8D). While the total numbers of tumor-infiltrating CD68+ macrophages and CD163+ M2 macrophages did not show significant differences between irradiated and unirradiated tumors, irradiated tumors contained a significant 5-fold increase in iNOS+ CD68+ macrophages than unirradiated tumors, resulting in a significantly increased M1:M2 ratio (Figure 8B). Within the rather small cohort of irradiated tumors, we did not observe any considerable impact of the irradiation dose on effector T cell infiltration, iNOS expression, vessel size, or infiltration by Treg. Thus, as in case of the murine RT5 tumor model, local LDI of human pancreatic cancer resulted in the accumulation of iNOS-positive intratumoral macrophages, reduced vessel size, and a strong accumulation of intraepithelial T cell infiltrates.

DISCUSSION

In this study, we demonstrate that local LDI of tumors (2 Gy) represents an efficient intervention to enable recruitment of tumor-reactive effector T cells into large, established murine as well as xenotransplanted and primary human tumors. Irradiation triggered the polarization of M2-like toward M1-like iNOS expressing tumor-associated macrophages. iNOS activity by these reprogrammed macrophages was exclusively responsible for the subsequent vascular normalization and activation, T cell recruitment, and tumor rejection. The critical role of iNOS+ macrophages is further emphasized by our finding that transfer of irradiated macrophages in combination with T cells also orchestrated vascular normalization, T cell infiltration, and tumor eradication. Thus, like local LDI, transfer of irradiated macrophages may also represent a promising adjuvant strategy for T cell-based cancer immunotherapy.

In previous studies, we have shown that normalization of the tumor vasculature is essential for efficient T cell infiltration (Hamzah et al., 2008). Interestingly, the radiation-induced vascular normalization observed here required not only the presence of irradiated macrophages but also the presence of tumor antigen-specific CD8+ T cells. These findings suggest a crosstalk between the macrophages and T cells resulting in modulation of the vasculature, e.g., through decreased VEGF production by macrophages and secretion of cytokines and chemokines with anti-angiogenic properties such as IFN-gamma, IP10, and MIG, which is in agreement with previous observations (Ganss et al., 2002).

Different macrophage subsets are known to be involved in the promotion and inhibition of tumorigenesis (Murray and Wynn, 2011). TAMs include M2-like macrophages, regulatory macrophages, and immature myeloid cells that together most likely represent a spectrum of M2-like activated phenotypes that functionally adapt to variable signals within the tumor microenvironment. They all suppress adaptive, tumor-specific immune responses, promote tumor growth and invasion, promote angiogenesis, and shape vascular morphology (Murray and Wynn, 2011; Stockmann et al., 2008; Sutterwala et al., 1998). In our study, adoptive T cell therapy alone did not result in tumor cell

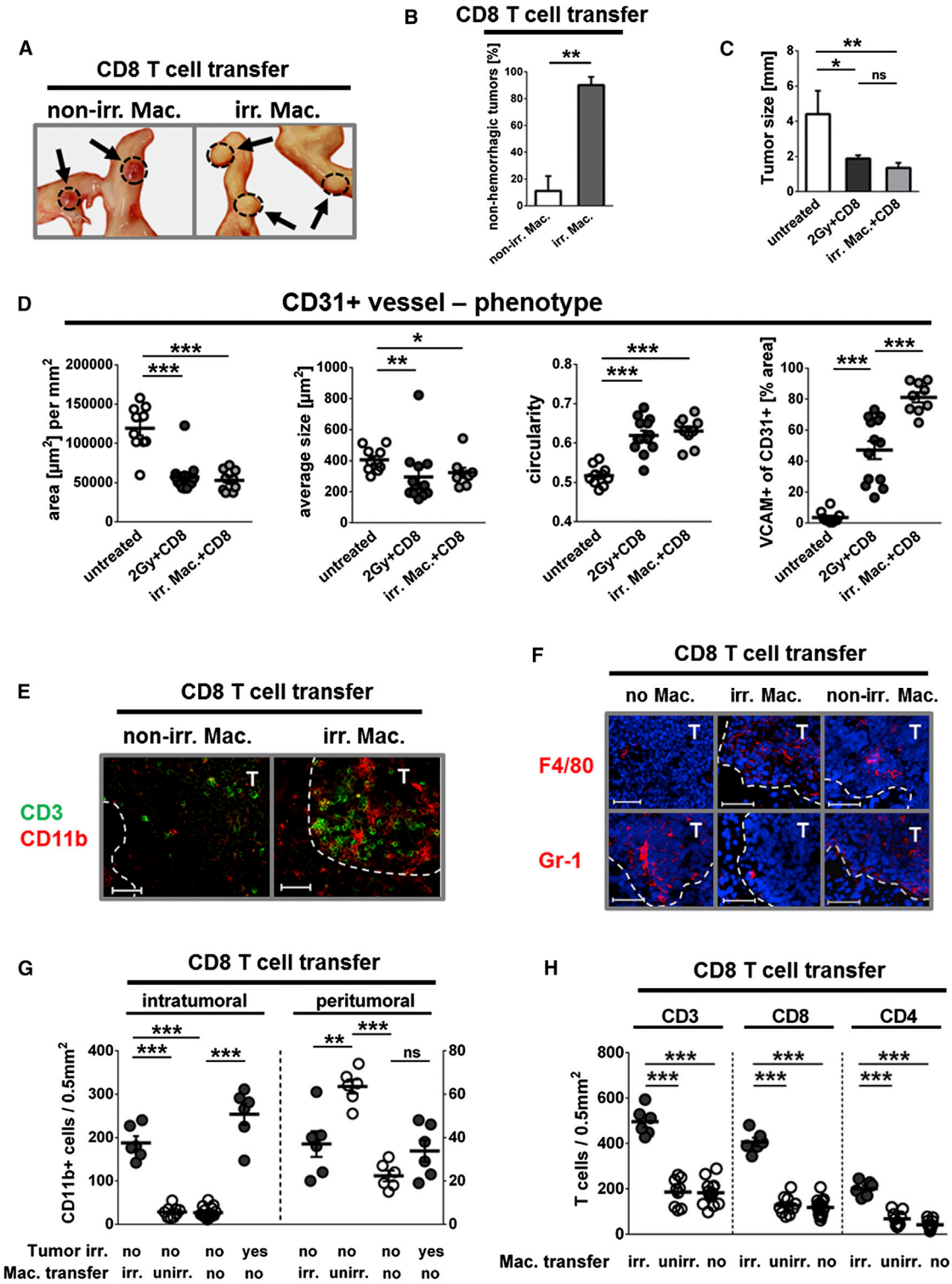

Figure 5. Irradiated Macrophages Are Essential and Sufficient for T Cell Recruitment into Tumor Tissue

(A) Absence of hemorrhages in RT5 tumors treated with irradiated macrophages compared to mice treated with nonirradiated macrophages. Photographs of representative RT5 tumors (arrows) are shown.

(B) Mean ± SEM of the proportion of nonhemorrhagic tumors per animal of mice treated with TC (CD8) after transfer of nonirradiated or irradiated macrophages.

(C) Mean ± SEM tumor size of untreated mice, mice treated with LDI (2 Gy) + TC (CD8) and mice treated with TC (CD8) after transfer of irradiated macrophages. Individual groups consisted of four to seven mice with 5–11 tumors.

(legend continued on next page)

destruction and prolonged survival, but instead caused a TAM-mediated upregulation of TH2 cytokines, VEGF, and GM-CSF. TH2 cytokines are critically involved in M2 cell differentiation (IL-10); inhibition of TH1 cytokine secretion (IL-4, IL-10); recruitment, activation, or maintenance of myeloid suppressor cells (IL-9); and activation of growth-promoting signaling pathways in tumor cells (IL-6; Multhoff et al., 2011). VEGF is a key factor driving the formation of the typically aberrant tumor vasculature and thereby endothelial anergy (Motz and Coukos, 2011), while GM-CSF is an important mediator in the recruitment and maintenance of myeloid suppressor cells in tumor tissues (Bayne et al., 2012). Together, these factors are critically involved in tumor-promoting cancer inflammation and tumor progression (Allavena and Mantovani, 2012). Our results disclose a hitherto unrecognized, potentially adverse role of the adaptive cellular immune system and a potential caveat in current treatment strategies exploiting adoptive T cell transfer that deserves further investigation.

Due to their tumor-promoting effects the inhibition or deletion of trophic TAMs—e.g., through clodronate liposome treatment—is a currently discussed option for cancer immunotherapy (Allavena and Mantovani, 2012). While our findings support the detrimental role of TAMs in the (T cell-aided) establishment of a tumor-promoting, immunosuppressive microenvironment, depletion of TAMs failed to improve tumor rejection in the context of T cell-based therapy. On the contrary, clodronate treatment abrogated the essential normalization of the tumor vasculature induced by LDI. Our results show that polarization of M2 toward M1-like macrophages is a better option than mere depletion of all TAMs. We achieved macrophage reprogramming with either local LDI or adoptive transfer of irradiated macrophages, both of which resulted in an accumulation of iNOS$^+$ macrophages within intraepithelial tumor areas. Because the numbers of intratumoral macrophages were low in untreated tumors, both, direct irradiation effects on TAMs as well as recruitment of co-irradiated macrophages from peritumoral areas of the pancreas, may have contributed to this accumulation. Both, local irradiation and the transfer of irradiated macrophages, were associated with a strong, NO-dependent induction of VCAM-1 on the tumor vasculature, which is likely to support recruitment of T cells and also macrophages into the tumor (Hyduk and Cybulsky, 2009; Ley et al., 2007).

M1 macrophages have been described to promote TH1 responses, support vascular normalization (Rolny et al., 2011), improve T cell recruitment (Johansson et al., 2012), and suppress the activities of M2 macrophages (Murray and Wynn, 2011; Gordon and Taylor, 2005). To date, the mechanisms of how M1 macrophages inhibit TAM-associated, tumor-promoting functions are only incompletely understood. TAM activity may be reversed by IFN-gamma (Murray and Wynn, 2011) but other mechanisms may be essential. We demonstrate that iNOS-positive macrophages in the tumor inhibited the production of most of the TAM-associated factors. NO has been introduced as an effector molecule of immunosuppressive myeloid suppressor cells with inhibitory activity on migration and survival of tumor-infiltrating T cells (Gabrilovich and Nagaraj, 2009). However, NO does not always act as a suppressive molecule in tumors as demonstrated by our findings that NO can also function as a key effector molecule of M1 polarized macrophages and thereby constitute an essential component of successful tumor immune rejection. It is possible that the cellular source or amount of NO are critical for its suppressive versus stimulatory capacity in the complex composition of the tumor microenvironment. Whereas irradiation of macrophages induced iNOS and downregulated the expression of molecules that convey an M2 phenotype, including Ym-1, Fizz1, and arginase (Gordon and Martinez, 2010), it did not increase iNOS expression in immunosuppressive Gr-1$^+$ myeloid cells. This observations suggests that irradiation, e.g., through DNA damage or inflammasome activation (Tesniere et al., 2008), selectively induced in macrophages a stress-related, proinflammatory translational program.

We investigated the role of LDI in the recruitment of T cells into both murine and human tumor tissues of different origin and at different sites. In all tested conditions, LDI was required for efficient T cell recruitment into tumor tissue and, where assessed, it was associated with the accumulation of iNOS-positive intraepithelial macrophages. This was also true for highly aggressive, locally advanced human pancreatic adenocarcinomas in which neoadjuvant local LDI induced an intraepithelial accumulation of CD4$^+$ and CD8$^+$ T cells and iNOS$^+$ macrophages as early as 3 days after irradiation, but a more extensive study with a larger number of patients is warranted for pancreatic ductal adenocarcinoma and other tumor types. Because the majority of patients with pancreatic cancer harbor expanded populations of spontaneously induced, tumor-reactive CD4$^+$ and CD8$^+$ effector and memory T cells in the blood and bone marrow (Schmitz-Winnenthal et al., 2005), local LDI might provide the possibility to recruit them to the tumor site and improve local antitumor immunity. Although we cannot exclude the possibility that such treatment may result in different outcomes when applied to other tumor

(D) Phenotype of CD31$^+$ vessels. Area per square millimeter, average size, circularity, and vessel activation status defined by VCAM + CD31$^+$ vessels, of CD31$^+$ tumor vessels in untreated mice (analyzed tumors = 10), mice treated with LDI (2 Gy) and TC (CD8) (analyzed tumors = 13) and mice treated with TC (CD8) after transfer of irradiated macrophages (analyzed tumors = 9). Individual groups consisted of two mice.

(E) Increased infiltration of myeloid CD11b$^+$ and transferred CD3$^+$ T cells in intratumoral areas of RT5 tumors treated with irradiated compared to non-irradiated macrophages analyzed with IHC using respective monoclonal antibodies. Tumor areas are indicated (T) and delineated (dashed lines). Scale bar, 50 μm.

(F) Infiltration of RT5 tumors with F4/80 and Gr-1$^+$ myeloid cells after CD8$^+$ T cell transfer without previous macrophage transfer or after transfer of irradiated or nonirradiated macrophages. Tumor areas are indicated (T) and delineated (dashed lines). Scale bar, 50 μm.

(G) Quantitative analysis of CD11b$^+$ cell infiltration in intratumoral (left) or peritumoral (right) areas after transfer of irradiated (analyzed tumors = 6) or nonirradiated (analyzed tumors = 6–9) macrophages or after local 2 Gy (analyzed tumors = 6) or no tumor (analyzed tumors = 6–15) irradiation. Individual groups consisted of five mice.

(H) Quantitative analysis of CD3$^+$, CD8$^+$, and CD4$^+$ intratumoral T cell infiltration after transfer of irradiated (analyzed tumors = 6) or nonirradiated (analyzed tumors = 9) macrophages or no tumor (analyzed tumors = 15) irradiation. Individual groups consisted of five mice. Mean ± SEM is shown. *$p < 0.05$; **$p < 0.01$; ***$p < 0.001$ (two-tailed Student's t test).

See also Figure S4.

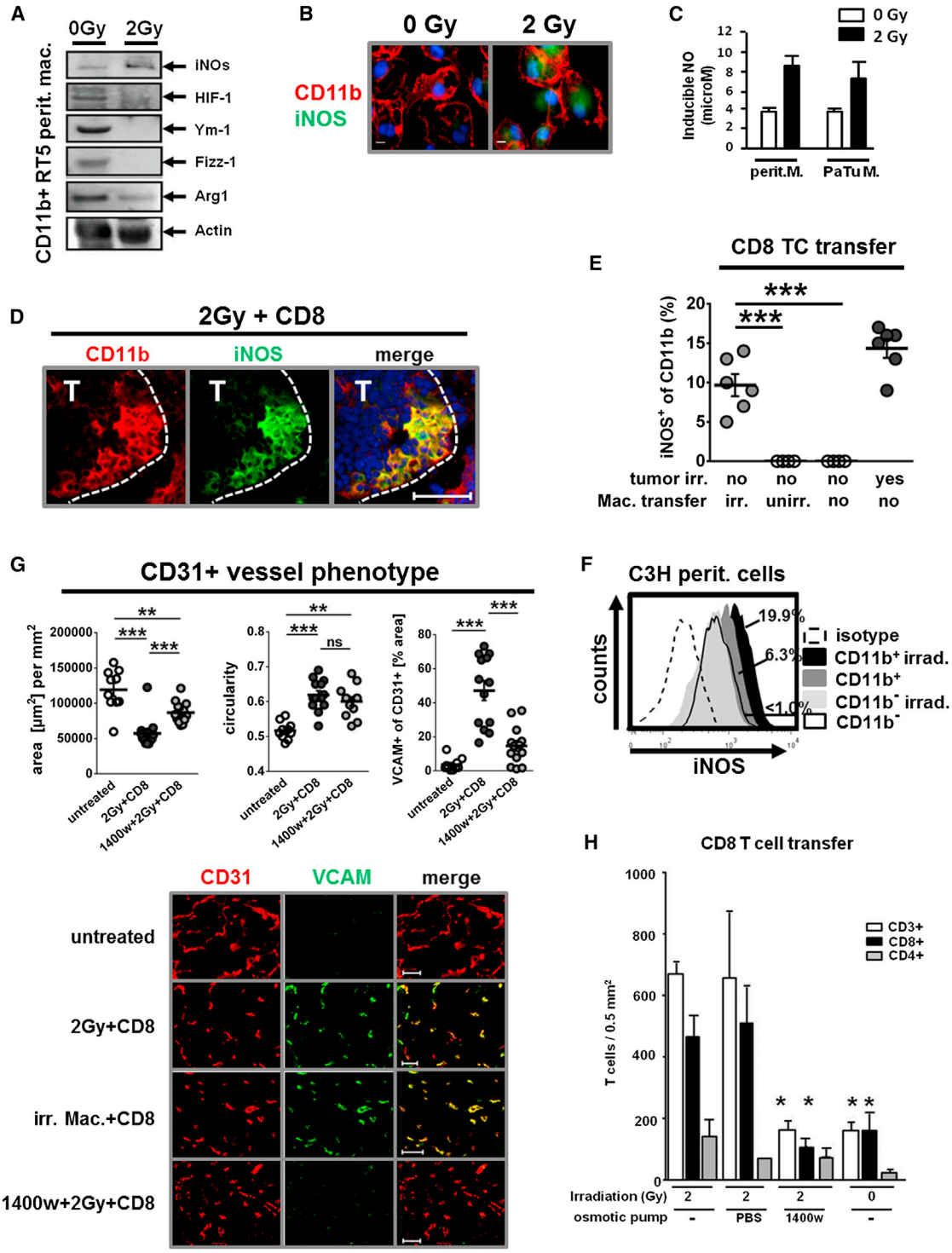

Figure 6. T Cell Recruitment Depends on Irradiation-Induced iNOS Expression

(A) Western blot analysis of isolated CD11b+ peritoneal macrophages derived from irradiated (2 Gy total body irradiation) or unirradiated (0 Gy) tumor-bearing RT5 mice.

(B) Immunocytological analysis of iNOS expression (green) in peritoneal MAC-1 (red)-positive macrophages of RT5 mice subjected to in vitro irradiation with 2 Gy 24 hr before analysis. Scale bar, 10 µm.

(C) Inducible NO secretion by irradiated (black bars) or unirradiated (white bars) peritoneal or tumor-infiltrating macrophages from RT5 mice analyzed 24 hr after irradiation.

(D) IHC analysis of iNOS (green) expression in CD11b+ (red) tumor-infiltrating macrophages within irradiated (2 Gy) RT5 tumors. Tumor areas are indicated (T) and delineated (dashed lines).

(legend continued on next page)

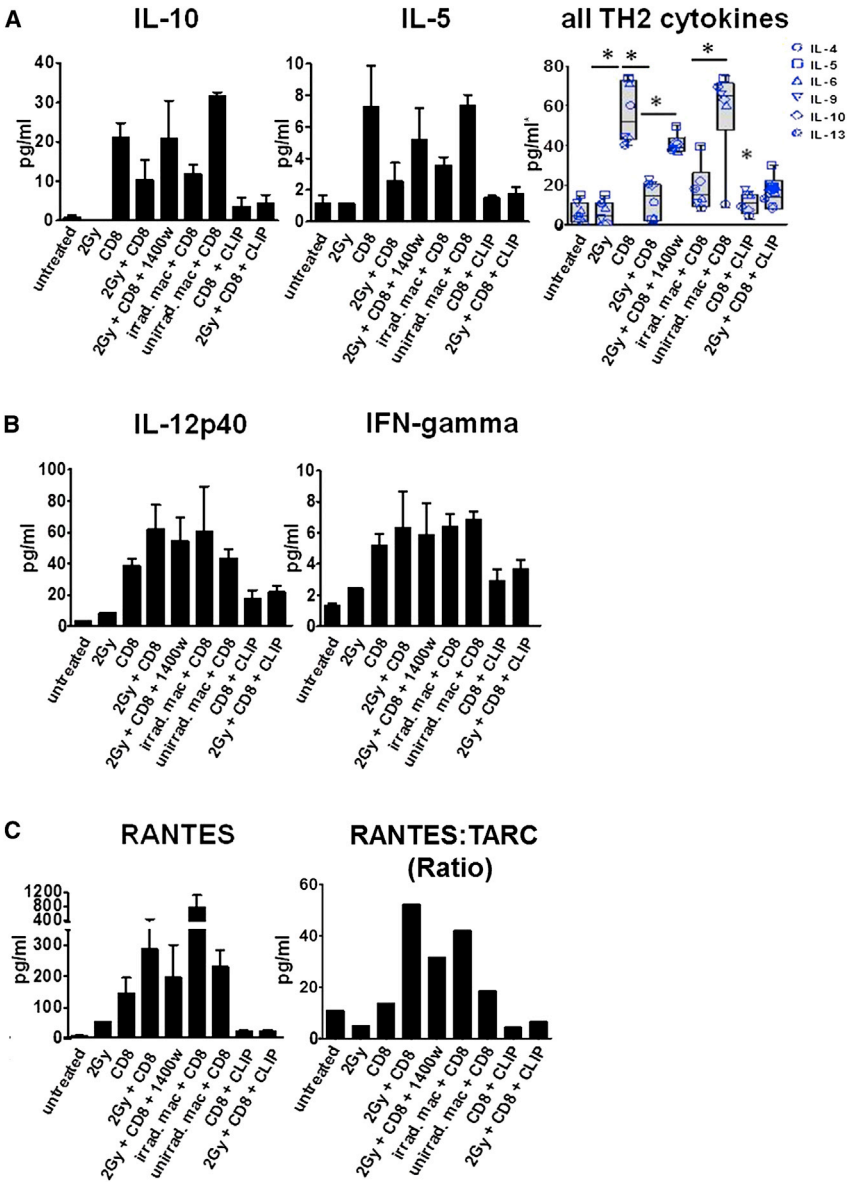

Figure 7. Irradiated Macrophages Control Tumorigenic Cancer Inflammation through iNOS

Mean concentrations of indicated TH2 (A) and TH1 (B) cytokines and RANTES (C) in RT5 tumor tissue lysates from 24-week-old RT5 mice are shown. RT5 tumors were isolated as indicated from untreated mice or from mice treated with LDI (2 Gy) or TCRCD8+ T cells (CD8) or with LDI + TCRCD8+ T cells (2 Gy + CD8). Some mice were additionally treated with iNOS inhibitor (2 Gy + CD8 + 1400W), received transfers of either irradiated or nonirradiated macrophages in combination with TCRCD8+ T cells, or were treated with CLIP. Error bars show SEM from resected RT5 tumors of two to seven animals. (A) Results of two representative TH2 cytokines are shown in the left and middle graphs. Cumulative data of all tested TH2 cytokines are shown in the right graph as mean values per test group (blue symbols) and box and whisker plot indicating mean ± minimum to maximum values of individual cytokines in each group. Cytokine concentrations in the right graph were adjusted by the following factors: IL-4 and IL-5, no adjustment; IL-6, × 1.6; IL-9 and IL-10, × 0.2; IL-13, and × 0.5. (C) The right graph shows the respective ratios of the concentrations of RANTES and CCL17.
See also Figure S6.

types, our study suggests that the described therapeutic interventions of either local LDI or, alternatively, the adoptive transfer of iNOS-expressing macrophages represent promising treatment options of broader applicability for combination with cancer immunotherapy. Whereas local LDI can only be applied to macroscopic tumors or metastases, adoptive transfer of activated macrophages may provide the advantage of targeting early microscopic tumor lesions systemically.

EXPERIMENTAL PROCEDURES

Mice

RT5 mice (Hanahan, 1985) were provided by D. Hanahan and the F1 generation of RT5/C3H mice was used (Garbi et al., 2004). TCRtg mice expressing MHC class I (H2-Kk; Garbi et al., 2004), (TCRCD8+) or II (H2-ABk; Garbi et al., 2004) (TCRCD4+) restricted Tag-derived epitopes SEFLLEKRI and TNRFNDLLDRMDIMFGSTGSADI (Garbi et al., 2004), and female NOD/SCID γ (NSG, NOD.Cg-*Prkdc*^{SCID}*Il2rgt*^{m1Wjl}/SzJ) mice were purchased from the animal facility of the DKFZ. Six- to eight-week-old female NOD/SCID mice (NOD/NCrCrl-*Prkdc*^{SCID}) and C3HeB/Fe mice were purchased from Charles River WIGA. All mice were kept under specific pathogen-free conditions at the German Cancer Research Center. Animal experiments were authorized by the local government (Regierungspräsidium Karlsruhe, Germany).

(E) Quantitative analysis of iNOS expression in intratumoral CD11b+ cells of irradiated (analyzed tumors = six) or non-irradiated (analyzed tumors = six) macrophages or after local 2 Gy (analyzed tumors = six) or no tumor (analyzed tumors = six) irradiation. Individual groups consisted of five mice.
(F) iNOS expression by indicated peritoneal cell populations isolated from untreated or irradiated C3H mice (n = 21) as analyzed by flow cytometry. Numbers indicate proportions of iNOS-expressing cells within respective populations.
(G) Phenotype of CD31+ vessels. Upper panel: area per square millimeter, circularity, and vessel activation status—defined by VCAM + CD31+ vessels—of CD31+ tumor vessels in untreated mice (analyzed tumors = 10), mice treated with LDI (2 Gy) + TC (CD8; analyzed tumors = 13) and mice treated with LDI (2 Gy) + TC (CD8) + 1400W (analyzed tumors = 10). Individual groups consisted of two mice. Lower panel: vessel structure (CD31) and activation status (VCAM) of tumors from untreated mice, mice treated with LDI (2 Gy) and TC (CD8), mice treated with TC (CD8) after transfer of irradiated macrophages, and mice treated with LDI (2 Gy) + TC (CD8) + 1400W. Scale bar, 50 μm. Mean ± SEM are shown. *$p < 0.05$; **$p < 0.01$; ***$p < 0.001$ (two-tailed Student's t test).
(H) Tumor infiltration by transferred TCRCD8+ T cells into 2 Gy irradiated RT5 animals treated with iNOS inhibitor 1400w or PBS as control through osmotic pumps or left untreated (n = 7 per group). Tumors were analyzed by IHC for presence of indicated T cell subsets.
See also Figure S5.

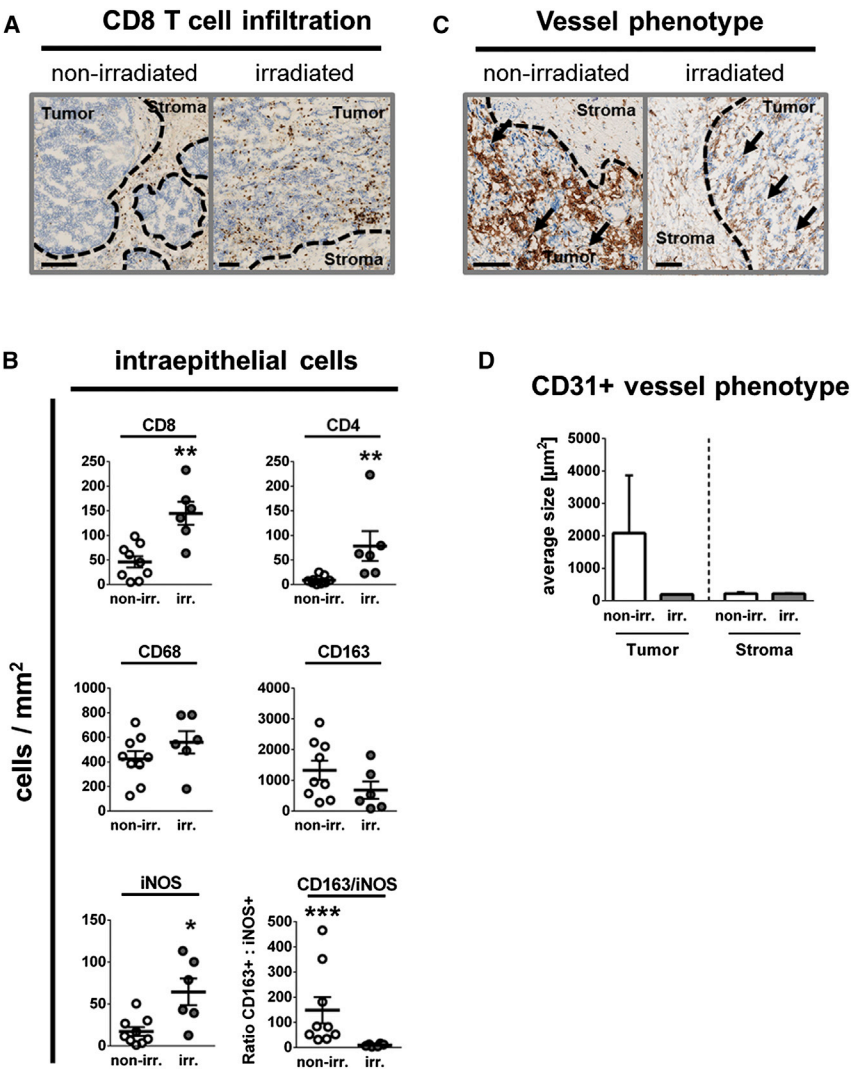

Figure 8. Local LDI Triggers Intraepithelial Accumulation of CD8+ and CD4+ T Cells and the Phenotype of CD31+ Vessels in Human Pancreatic Cancer

(A) Increased intraepithelial CD8+ T cell infiltration (brown staining) in irradiated human pancreatic carcinomas in contrast with peritumoral T cell infiltration in non-irradiated tumors. Nuclei are counterstained with Hemalaun (blue). Scale bar, 100 μm.

(B) Infiltration of indicated immune cell populations in intraepithelial areas of human pancreatic tumors as assessed by IHC. Dots represent values of individual patients. Mean values are depicted by horizontal lines.

(C) Reduced CD31 vessel size (brown staining) in irradiated human pancreatic carcinomas in comparison with nonirradiated tumors. Nuclei are counterstained with Hemalaun (blue). Tumor and stroma areas are delineated by dashed lines. Scale bar, 100 μm.

(D) Mean ± SEM of the average CD31+ vessel size from irradiated (n = 6) and nonirradiated (n = 9) patients in the tumor and stroma. *p < 0.05; **p < 0.01; ***p < 0.001 (Mann-Whitney U test).

Tumor Allografts

RT5 tumors were isolated from RT5 mice and transplanted into dorsal skin folds of NOD/SCID mice. Animals were monitored regularly for tumor growth. Mice bearing tumors larger than 64 mm^3 were selected for further experiments. In some experiments 7- to 9-week-old female NSG mice were engrafted with cells of the human melanoma line MeWo i.d. (2.5×10^6 cells in 50 μl of Matrigel [BD Biosciences]) on the right hind leg.

Irradiation

Twenty-four-week-old RT5 mice were anesthetized and irradiated with 0.5, 1, 2, or 6 Gy with a Gammatron Cobalt 60 therapy unit (Siemens). Irradiation was directed at the pancreatic region by shielding caudal and cranial areas using a 3 mm lead apron. Tumors in NOD/SCID and NSG mice were locally irradiated with 2 Gy using the same therapy unit. In some experiments, mice were splenectomized (Feuerer et al., 2003). Afterward the animals were left to rest for 10 days before experiments were conducted.

Vaccination

MHC class I restricted SV40-Tag peptide (Genomics and Proteomics Core Facility of the German Cancer Research Center; SEFLLEKRI; 50 μg) was emulsified in CFA (Sigma) in a total volume of 200 μl (v/v 1:1) and injected under the neck skin of RT5 mice 1 week before local tumor irradiation. Some mice received additional boosting immunizations 1 week after irradiation. Tumors were excised 1 week thereafter and analyzed.

Adoptive Cell Transfer

Murine T cell transfer was conducted as described (Garbi et al., 2004); for more details, see Supplemental Experimental Procedures.

Macrophage Transfer

Eight- to 12-week-old, sex-matched C3H donor mice received a 2 Gy TBI or were left unirradiated. After 1 day, 1 ml of thioglycolate (3%, AppliChem; Marley et al., 1995) were injected intraperitoneally (i.p.). Peritoneal macrophages were collected by peritoneal lavage after 3 days and 5×10^6 doses were injected i.v. into each recipient mouse.

Macrophage Analyses

CD11b+ peritoneal and intratumoral macrophages were isolated by peritoneal lavage or from single tumor cell suspensions with MACS-based separation (CD11b mAb M1/70, Miltenyi), cultured overnight in RPMI medium containing 10% FCS, washed, and irradiated with 2 Gy. Twenty-four hours later, culture supernatants were analyzed for production of nitric oxide (Griess reagent method; Sigma) and macrophages were either analyzed by immunocytology or lysed in RIPA buffer (Sigma) and subjected to western blot analysis using primary rabbit anti-mouse Abs against iNOS, arginase-1, β-actin (BD PharMingen), Ym-1 (Stem Cell Technology), Fizz-1 (Abcam), and HIF-1 (Novus Biologicals); and horseradish peroxidase-conjugated, secondary goat anti-rabbit antibodies (Sigma). Blots were developed with ECL reagent (GE Healthcare).

Clodronate Treatment

Clodronate (Roche Diagnostics) was encapsulated in liposomes (N. van Rooijen, VUMC) to create CLIP. Control liposomes contained PBS. The 200 μl clodronate-encapsulated liposomes (Encapsula NanoSciences or N. van Rooijen, VUMC) were initially injected i.p., then 100 μl every 5 days over 3 weeks for the duration of the experiment.

iNOS Inhibition

The selective iNOS inhibitor 1400W (Tocris Bioscience) was released at a concentration of 240 μg/μl in 200 μl PBS using an ALZET mini-osmotic pump (ALZET Osmotic Pumps) placed under the dorsal skin providing 6 mg/kg/hr over 2 weeks.

Cytokine Analyses

RT5 tumor tissue was lysed using the Bio-Plex Cell Lysis Kit (Bio-Rad) and processed as described previously (Domschke et al., 2009). Cytokines were quantified using the multiplex protein array system technology (Bio-Rad Laboratories) according to the manufacturer's protocol (R&D Systems).

1400W Efficacy

RT5 tumor lysates were filtered using Amicon Ultra 0.5 ml centrifugal filters (Millipore) and analyzed using the Nitrate/Nitrite Fluorometric Assay Kit (Cayman Chemical).

Human Samples

Samples from local, advanced pancreatic tumors that were resected 3 days after a single local LDI with 0.5–5 Gy (n = 6; Timke et al., 2011) or left unirradiated (n = 9) were obtained after informed consent. The study was approved by the ethic committee of the University Heidelberg (NCT01027221). Clinical studies were approved by local and governmental authorities.

Immunohistology/Cytology

Murine tumors were embedded in OCT compound, snap-frozen, sectioned (Leica CM1950, Leica Biosystems), stained with hematoxylin-eosin or different antibodies. Human pancreatic tumors were sectioned and stained as described previously (Halama et al., 2011). Antibody and staining details are provided in the Supplemental Experimental Procedures.

Statistical Analyses

The p values were calculated with the two-sided Student's t test or the Mann-Whitney U test. The Mantel-Cox test was used for survival calculations. A p value < 0.05 was considered significant. Tumor growth experiments were tested with Spearman's rank correlation. A threshold value of r was set at -0.5 to indicate a significant difference in the case of blood glucose decrease.

SUPPLEMENTAL INFORMATION

Supplemental Information includes Supplemental Experimental Procedures and six figures and can be found with this article online at http://dx.doi.org/10.1016/j.ccr.2013.09.014.

ACKNOWLEDGMENTS

The work was supported by the Deutsche Forschungsgemeinschaft (SFB938), and G.J.H. was supported by the Wilhelm Sander-Stiftung.

Received: November 21, 2012
Revised: April 30, 2013
Accepted: September 19, 2013
Published: October 24, 2013

REFERENCES

Allavena, P., and Mantovani, A. (2012). Immunology in the clinic review series; focus on cancer: tumour-associated macrophages: undisputed stars of the inflammatory tumour microenvironment. Clin. Exp. Immunol. *167*, 195–205.

Antonia, S., Mulé, J.J., and Weber, J.S. (2004). Current developments of immunotherapy in the clinic. Curr. Opin. Immunol. *16*, 130–136.

Bayne, L.J., Beatty, G.L., Jhala, N., Clark, C.E., Rhim, A.D., Stanger, B.Z., and Vonderheide, R.H. (2012). Tumor-derived granulocyte-macrophage colony-stimulating factor regulates myeloid inflammation and T cell immunity in pancreatic cancer. Cancer Cell *21*, 822–835.

Cao, Z.A., Daniel, D., and Hanahan, D. (2002). Sub-lethal radiation enhances anti-tumor immunotherapy in a transgenic mouse model of pancreatic cancer. BMC Cancer *2*, 11.

De Monte, L., Reni, M., Tassi, E., Clavenna, D., Papa, I., Recalde, H., Braga, M., Di Carlo, V., Doglioni, C., and Protti, M.P. (2011). Intratumor T helper type 2 cell infiltrate correlates with cancer-associated fibroblast thymic stromal lymphopoietin production and reduced survival in pancreatic cancer. J. Exp. Med. *208*, 469–478.

Domschke, C., Schuetz, F., Ge, Y., Seibel, T., Falk, C., Brors, B., Vlodavsky, I., Sommerfeldt, N., Sinn, H.P., Kühnle, M.C., et al. (2009). Intratumoral cytokines and tumor cell biology determine spontaneous breast cancer-specific immune responses and their correlation to prognosis. Cancer Res. *69*, 8420–8428.

Feuerer, M., Beckhove, P., Garbi, N., Mahnke, Y., Limmer, A., Hommel, M., Hammerling, G.J., Kyewski, B., Hamann, A., Umansky, V., and Schirrmacher, V. (2003). Bone marrow as a priming site for T-cell responses to blood-borne antigen. Nat. Med. *9*, 1151–1157.

Fridman, W.H., Galon, J., Pagès, F., Tartour, E., Sautès-Fridman, C., and Kroemer, G. (2011). Prognostic and predictive impact of intra- and peritumoral immune infiltrates. Cancer Res. *71*, 5601–5605.

Gabrilovich, D.I., and Nagaraj, S. (2009). Myeloid-derived suppressor cells as regulators of the immune system. Nat. Rev. Immunol. *9*, 162–174.

Ganss, R., and Hanahan, D. (1998). Tumor microenvironment can restrict the effectiveness of activated antitumor lymphocytes. Cancer Res. *58*, 4673–4681.

Ganss, R., Ryschich, E., Klar, E., Arnold, B., and Hämmerling, G.J. (2002). Combination of T-cell therapy and trigger of inflammation induces remodeling of the vasculature and tumor eradication. Cancer Res. *62*, 1462–1470.

Garbi, N., Arnold, B., Gordon, S., Hämmerling, G.J., and Ganss, R. (2004). CpG motifs as proinflammatory factors render autochthonous tumors permissive for infiltration and destruction. J. Immunol. *172*, 5861–5869.

Garvey, E.P., Oplinger, J.A., Furfine, E.S., Kiff, R.J., Laszlo, F., Whittle, B.J., and Knowles, R.G. (1997). 1400W is a slow, tight binding, and highly selective inhibitor of inducible nitric-oxide synthase in vitro and in vivo. J. Biol. Chem. *272*, 4959–4963.

Gordon, S., and Taylor, P.R. (2005). Monocyte and macrophage heterogeneity. Nat. Rev. Immunol. *5*, 953–964.

Gordon, S., and Martinez, F.O. (2010). Alternative activation of macrophages: mechanism and functions. Immunity *32*, 593–604.

Griffioen, A.W., Damen, C.A., Blijham, G.H., and Groenewegen, G. (1996). Tumor angiogenesis is accompanied by a decreased inflammatory response of tumor-associated endothelium. Blood *88*, 667–673.

Halama, N., Michel, S., Kloor, M., Zoernig, I., Benner, A., Spille, A., Pommerencke, T., von Knebel, D.M., Folprecht, G., Luber, B., et al. (2011). Localization and density of immune cells in the invasive margin of human colorectal cancer liver metastases are prognostic for response to chemotherapy. Cancer Res. *71*, 5670–5677.

Hamzah, J., Jugold, M., Kiessling, F., Rigby, P., Manzur, M., Marti, H.H., Rabie, T., Kaden, S., Gröne, H.J., Hämmerling, G.J., et al. (2008). Vascular normalization in Rgs5-deficient tumours promotes immune destruction. Nature *453*, 410–414.

Hanahan, D. (1985). Heritable formation of pancreatic beta-cell tumours in transgenic mice expressing recombinant insulin/simian virus 40 oncogenes. Nature *315*, 115–122.

Hyduk, S.J., and Cybulsky, M.I. (2009). Role of alpha4beta1 integrins in chemokine- induced monocyte arrest under conditions of shear stress. Microcirculation *16*, 17–30.

Islam, S.A., and Luster, A.D. (2012). T cell homing to epithelial barriers in allergic disease. Nat. Med. *18*, 705–715.

Johansson, A., Hamzah, J., Payne, C.J., and Ganss, R. (2012). Tumor-targeted TNFα stabilizes tumor vessels and enhances active immunotherapy. Proc. Natl. Acad. Sci. USA *109*, 7841–7846.

Ley, K., Laudanna, C., Cybulsky, M.I., and Nourshargh, S. (2007). Getting to the site of inflammation: the leukocyte adhesion cascade updated. Nat. Rev. Immunol. *7*, 678–689.

Marley, S.B., Hadley, C.L., and Wakelin, D. (1995). Genetic variation in neutrophil accumulation in mice is not mediated through immigrant regulatory cells. Clin. Exp. Immunol. *102*, 224–228.

Motz, G.T., and Coukos, G. (2011). The parallel lives of angiogenesis and immunosuppression: cancer and other tales. Nat. Rev. Immunol. *11*, 702–711.

Multhoff, G., Molls, M., and Radons, J. (2011). Chronic inflammation in cancer development. Front. Immunol. *2*, 98.

Murray, P.J., and Wynn, T.A. (2011). Protective and pathogenic functions of macrophage subsets. Nat. Rev. Immunol. *11*, 723–737.

Nummer, D., Suri-Payer, E., Schmitz-Winnenthal, H., Bonertz, A., Galindo, L., Antolovich, D., Koch, M., Buchler, M., Weitz, J., Schirrmacher, V., and Beckhove, P. (2007). Role of tumor endothelium in CD4+ CD25+ regulatory T cell infiltration of human pancreatic carcinoma. J. Natl Cancer Inst. *99*, 1188–1199.

Rolny, C., Mazzone, M., Tugues, S., Laoui, D., Johansson, I., Coulon, C., Squadrito, M.L., Segura, I., Li, X., Knevels, E., et al. (2011). HRG inhibits tumor growth and metastasis by inducing macrophage polarization and vessel normalization through downregulation of PlGF. Cancer Cell *19*, 31–44.

Ryschich, E., Schmidt, J., Hammerling, G.J., Klar, E., and Ganss, R. (2002). Transformation of the microvascular system during multistage tumorigenesis. Int. J Cancer *97*, 719–725.

Schmitz-Winnenthal, F.H., Volk, C., Z'graggen, K., Galindo, L., Nummer, D., Ziouta, Y., Bucur, M., Weitz, J., Schirrmacher, V., Büchler, M.W., and Beckhove, P. (2005). High frequencies of functional tumor-reactive T cells in bone marrow and blood of pancreatic cancer patients. Cancer Res. *65*, 10079–10087.

St Croix, B., Rago, C., Velculescu, V., Traverso, G., Romans, K.E., Montgomery, E., Lal, A., Riggins, G.J., Lengauer, C., Vogelstein, B., and Kinzler, K.W. (2000). Genes expressed in human tumor endothelium. Science *289*, 1197–1202.

Stockmann, C., Doedens, A., Weidemann, A., Zhang, N., Takeda, N., Greenberg, J.I., Cheresh, D.A., and Johnson, R.S. (2008). Deletion of vascular endothelial growth factor in myeloid cells accelerates tumorigenesis. Nature *456*, 814–818.

Sutterwala, F.S., Noel, G.J., Salgame, P., and Mosser, D.M. (1998). Reversal of proinflammatory responses by ligating the macrophage Fcgamma receptor type I. J. Exp. Med. *188*, 217–222.

Tesniere, A., Apetoh, L., Ghiringhelli, F., Joza, N., Panaretakis, T., Kepp, O., Schlemmer, F., Zitvogel, L., and Kroemer, G. (2008). Immunogenic cancer cell death: a key-lock paradigm. Curr. Opin. Immunol. *20*, 504–511.

Timke, C., Winnenthal, H.S., Klug, F., Roeder, F.F., Bonertz, A., Reissfelder, C., Rochet, N., Koch, M., Tjaden, C., Buechler, M.W., et al. (2011). Randomized controlled phase I/II study to investigate immune stimulatory effects by low dose radiotherapy in primarily operable pancreatic cancer. BMC Cancer *11*, 134.

Voss, R.H., Thomas, S., Pfirschke, C., Hauptrock, B., Klobuch, S., Kuball, J., Grabowski, M., Engel, R., Guillaume, P., Romero, P., et al. (2010). Coexpression of the T-cell receptor constant alpha domain triggers tumor reactivity of single-chain TCR-transduced human T cells. Blood *115*, 5154–5163.

Zeisberger, S.M., Odermatt, B., Marty, C., Zehnder-Fjällman, A.H., Ballmer-Hofer, K., and Schwendener, R.A. (2006). Clodronate-liposome-mediated depletion of tumour-associated macrophages: a new and highly effective anti-angiogenic therapy approach. Br. J. Cancer *95*, 272–281.